Indian J. Phys. **73A** (2), 205–212 (1999)

IJP A
— an international journal

Composition dependence of electrical resistivity of bismuth antimonide thin films

P S Nikam* and R Y Borse+

P G Department of Physical Chemistry* and Department of Physics+,
M S G College, Malegaon Camp-423 105, Nasik, Maharashtra, India

Received 12 November 1997, accepted 22 June 1998

Abstract : Thin films of $Bi_{1-x}Sb_x$ of varying compositions and thicknesses have been formed on glass substrates employing three-temperature method. Electrical resistivity (ρ), activation energy (ΔE) and temperature coefficient of resistance (TCR) have been studied as a function of composition, thickness and temperature of the film The films of $Bi_{1-x}Sb_x$ ($0 < x \leq 0.42$) show semiconducting behaviour and ($x > 0.42$) show semiconducting behaviour in low temperature region and metallic behaviour in high temperature region.

Keywords : Thin films of $Bi_{1-x}Sb_x$, electrical resistivity, temperature coefficient of resistance

PACS Nos. : 73.50.-h, 73.61.-r

1. Introduction

Bi-Sb alloys are interesting from the physics point of view because they can exhibit semi-metallic, semiconducting or gapless characteristics, depending on the percentage of Sb. They are also useful because Bi-Sb alloys with less than 20% Sb have potential for efficient thermoelectric conversion [1]. Survey of literature shows that the study of electrical properties of Bi-Sb system in thin film state [2–4] over the entire range of composition is scanty. Since the composition of deposits affect the transport properties critically, it is felt necessary to study in detail the transport properties of Bi-Sb films of varying composition.

2. Experimental

Thin films of $Bi_{1-x}Sb_x$ were prepared by three-temperature method [5,6]. Bismuth and antimony (purities 99.999%) were evaporated directly from separate preflashed conical

© 1999 IACS

baskets of nichrome wire. The evaporation was done at room temperature on gold seal microscope glass slides in an IBPTORR-120 vacuum unit, under a vacuum of the order of 10^{-5} torr. Both elements were simultaneously evaporated. After adjusting the flux rates from the two sources by varying the source current, films of varying compositions and different thicknesses were obtained. The films were subsequently annealed at 150°C for 6 hrs in vacuum.

The method employed to determine the composition, thickness and uniformity of the film were similar to those reported earlier [7,8]. The composition of the film was determined by employing absorption spectroscopy [9] at wavelength of 550 mµ with an accuracy of ±1 at. %.

Antimony is initially present in trivalent form. To determine the composition of antimony (Sb) colorimetrically, antimony is to be oxidized, Sb(III) to Sb(V) [trivalent to pentavalent]. The Bi-Sb films after measurements are weighed accurately, and dissolved in 5 ml concentrated H_2SO_4 and diluted to 100 ml with distilled water to make 3N solution. This acts as stock solution. This stock solution contains trivalent Sb. This trivalent antimony is oxidized to pentavalent as described by Charlot [9]. The amount of Sb(V) is then quantitatively estimated colorimetrically by using optical filter of 550 mµ wavelength.

Film thickness (d) was measured by gravimetric method [7,8,10] using the relation,

$$d = \frac{M}{g \times A} \text{ cm}, \tag{1}$$

where A is surface area of the film, M, the mass of the film and g, the density of the film material expressed as

$$g = x_1 g_1 + x_2 g_2, \tag{2}$$

where g_1, g_2 and x_1, x_2 are densities and atomic fractions of Bi and Sb elements respectively. Film thickness (d) was also measured by multiple beam interferometry. Both techniques of thickness measurements agreed within ± 10% for very thin films and ± 50% for thick films (> 500 Å). Films prepared for electrical measurements have composition ranging between $Bi_{15}Sb_{85}$ and $Bi_{95}Sb_{05}$ and thickness between 800 and 9990 Å. Electrical resistances of the films were measured at various temperatures in vacuum using pressure contacts [7,8,11,12]. This avoided the contamination of films.

3. Results and discussion

Figure 1 shows the variation of log R *versus* $1/T$ for $Bi_{1-x}Sb_x$ ($0 < x \leq 0.42$) films. It is seen from the figure that $Bi_{1-x}Sb_x$ ($0 < x \leq 0.42$) films exhibit semiconducting behaviour between 303 to 443 K. Mikolajczak *et al* [4] too reported the semiconducting behaviour of $Bi_{1-x}Sb_x$ ($0 < x \leq 0.42$) films. The energy of avtivation (ΔE) values calculated from slopes of

graph in Figure 1 reveal that the activation energy (ΔE) appears to have a maximum value at a concentration near 5 at. % of Sb. The variation of ΔE with composition of these

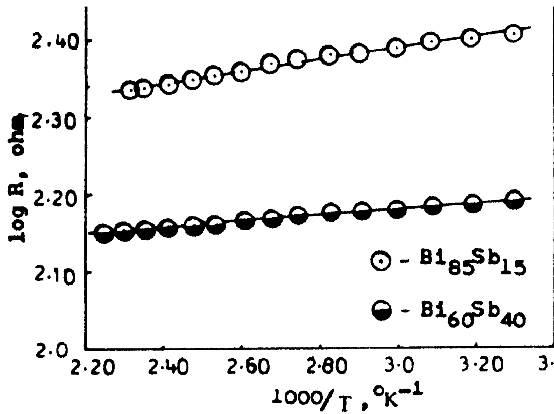

Figure 1. Plot of log R *versus* $1/T$ of $Bi_{1-x}Sb_x$ $(0 < x \leq 0.42)$ film

semiconducting films is shown in Figure 2. It can be said further that with an increase in concentration of Sb in Bi, the band gap in Bi decreases rapidly.

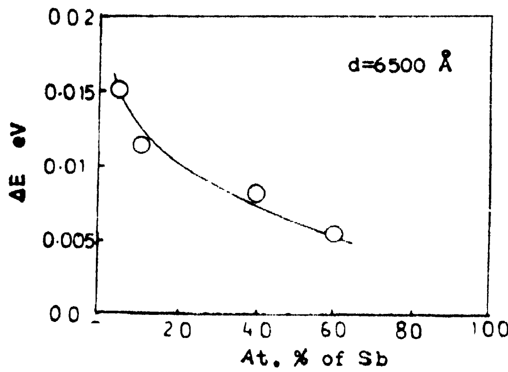

Figure 2. Plot of activation energy (ΔE) *versus* at.% of Sb in $Bi_{1-x}Sb_x$ films.

Figure 3 includes the variation of ΔE *versus* thickness (d) of the semiconducting $Bi_{1-x}Sb_x$ $(0 < x \leq 0.42)$ films. As expected ΔE decreases with increase of thickness of the film

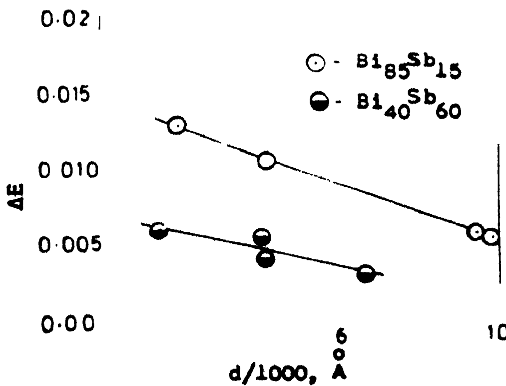

Figure 3. Plot of activation energy (ΔE) *versus* thickness of $Bi_{1-x}Sb_x$ films.

which could be explained on the assumptions [13] of the change in barrier height due to the size of grain in a polycrystalline film [14], large dislocations of crystals, size effects and change in the stoichiometry. The inverse relation between ΔE and thickness of these films could also be explained on island structure theory of Neugebauer [15,16].

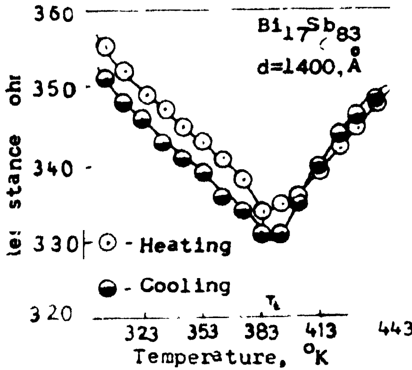

Figure 4. Plot of resistance *versus* temperature of $Bi_{1-x}Sb_x$ ($x > 0.42$) film.

Figure 4 shows the variation of resistance with temperature for $Bi_{1-x}Sb_x$ ($x > 0.42$) films. It is seen from this figure that $Bi_{1-x}Sb_x$ ($x > 0.42$) films exhibit semiconducting behaviour in the low temperature region (~300 to 383 K) and metallic in high temperature region (383 to 443 K). The temperature of transition from semiconducting to metallic nature is ~383 K during the heating and cooling of the film. The transition temperature does not change with thickness and composition of the films. Energy of activation values of $Bi_{1-x}Sb_x$ ($x > 0.42$) films in semiconducting region are illustrated in Figure 3. It is observed from figure that ΔE values decrease with increase of film thickness. The dependence of ΔE values on thickness of $Bi_{1-x}Sb_x$ ($x > 0.42$) films could be well explained with Slater and Neugebauer model as has been done by Nikam and Aher [17].

$Bi_{1-x}Sb_x$ ($x > 0.42$) films exhibit metallic behaviour in high temperature region (383 to 443 K). Metallic thin films, due to their structural features and size effects, have properties somewhat different from those of bulk materials. The electrical resistivity, ρ, of thin metallic films can be expressed by FS theory [18] as,

$$\rho = \rho_0\left[1+\frac{3l_0}{8d}(1-p)\right], \tag{3}$$

where ρ is the electrical resistivity of the film; ρ_0, the electrical resistivity of bulk material; l_0, the mean free path of electron; d, the film thickness and p is the specularity parameter.

The experimentally measured resistivity of thin films as shown by Mayadas and Shatzkes [19] is dependent not only on the ordinary Fuchs size effect but also on the effect of grain boundary scattering. The thin film electrical resistivity given by MS for small α' is

$$\rho=\rho_0\left[1+3/2\alpha'+\frac{3l_0}{8d}(1-p)\right], \tag{4}$$

where $\alpha' = \dfrac{l_0 R'}{d(1-R')}$. Here d, the average grain diameter and R', the grain boundary reflection coefficient.

Figure 5 shows ρd as a function of d (using eq. 3). The intercept of this graph on y-axis yields $l_0(1-p)$ while the slope yields ρ_0 which is the electrical resistivity of an infinitely thick film.

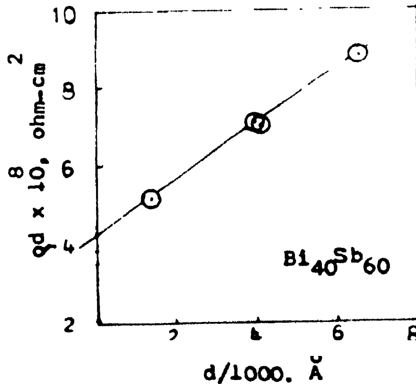

Figure 5. Plot of ρd *versus* thickness(d) of $Bi_{1-x}Sb_x$ films at high temperature (metallic behaviour)

Assuming $p = 0$ for total diffuse scattering, we obtain the value of l_0 as 15099 Å in $Bi_{1-x}Sb_x$ ($x > 0.42$) films. Assuming that the values of ρ_0 and $l_0(1-p)$ derived from Fuchs model are also appropriate for the MS model. Eq. 4 has been used for estimating the values of ρ_0 for two thicknesses, *viz*. 1400 and 4000 Å. Further the values of R' have been calculated on the assumption that the grain diameter approximately equals the film thickness. Data for ρ_0; l_0 and R' is given in Table 1.

Table 1. Data for ρ_0, l_0, α' and R' of $Bi_{1-x}Sb_x$ films

Thickness d, Å	$\rho \times 10^4$ ohm-cm	$\rho_0 \times 10^4$ ohm-cm	l_0 Å	α'	$R' \times 10^5$
1400	37.04	7.241	16000	2.7431	2.5435
4000	17.69	7.241	15000	0.9618	2.5651

Figure 6 shows the variation of ρ with thickness of the Bi-Sb films with excess Bi and excess Sb at room temperature. In both cases, resistivity ρ decreases with increase of film thickness. In thicker films, ρ remains almost constant. The increase of ρ for thinner films may be mostly due to island structure of the film. The effect of film thickness can also be explained on Matheissen rule,

$$\rho_{\text{total}} = \rho_{\text{ideal}} + \rho_{\text{residual}} + \rho_{\text{thickness}}, \tag{5}$$

where ρ_{ideal} depends on the amplitude of thermal motion of the ions, ρ_{residual}, the component strongly dependent on the lattice defects but independent of temperature as long as these lattice defects are not affected by the temperature change, and $\rho_{\text{thickness}}$, the component of

ρ_{total} that depends on the thickness of the film. Now as thickness of the film increases, effect of island structure, quantum size effect and defects like grain size *etc*. are diminished, thus

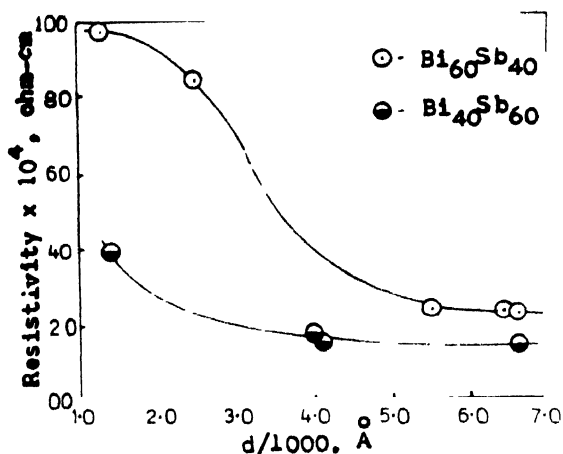

Figure 6. Plot of resistivity *versus* thickness of $Bi_{1-x}Sb_x$ films at room temperature.

reducing the contribution of $\rho_{thickness}$ on ρ_{total}. Contribution of ρ_{ideal} and $\rho_{residual}$ in ρ_{total} being characteristics of the materials. Thus, ρ_{total} of films decreases with the increasing film thickness.

The decrease of ρ in the semiconducting region with increase of thickness may be due to anomalous size effect. This effect was explained by the influence of surface bending of the film potential [20].

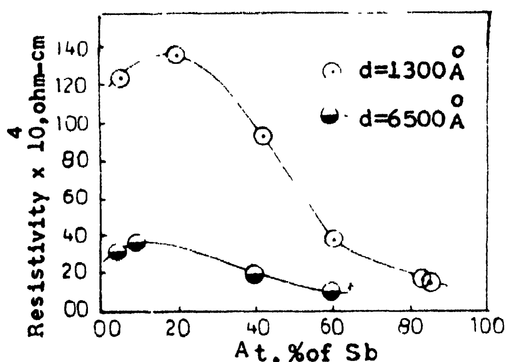

Figure 7. Plot of rsistivity *versus* at.% of Sb in $Bi_{1-x}Sb_x$ films.

The variation of ρ with at. % of Sb in Bi-Sb films at room temperature is shown in Figure 7. It is seen from this figure that the films of intermediate composition have high resistivity with a peak at around 10–20 at.% of Sb, which is probably due to the depletion of carriers in the films. The decrease on ρ with increase of Sb concentration beyond maxima is unexpected because it would be more natural for this parameter to increase with Sb concentration at low temperatures. Similar results for variation of ρ with at.% of Sb of Bi-Sb in thin film state have been reported [19].

Figure 8 shows the variation of temperature coefficient of resistance (TCR) with temperature of $Bi_{1-x}Sb_x$ film. It is found that TCR is negative for $Bi_{1-x}Sb_x$ $(0 < x \leq 0.42)$

films and its value decreased continuously with rise of temperature. The decrease in negative TCR with increase of temperature can be explained on the basis of island structure

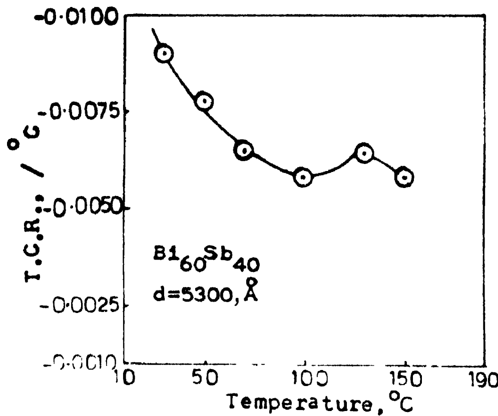

Figure 8. Plot of TCR *versus* temperature of $Bi_{1-x}Sb_x$ ($0 < x \leq 0.42$) film

concept proposed by Neugebauer and Weeb [16] and later developed by Neugebauer [15] to explain semiconducting behaviour of very thin films. The expression for negative TCR is given by Nikam and Mankar [21]

$$\text{Negative TCR} = \frac{-d(d)}{dT}\left[\frac{4\Pi\sqrt{2m\phi}}{h^2} + \frac{1}{d}\right] + \frac{C}{T^2}, \tag{6}$$

where $C = \dfrac{(2e^2/\varepsilon r) + \Delta E_g}{2K}$ (assuming that $\delta(\Delta E)/\delta T$ and $\delta\phi/\delta T$ is zero); d, the average distance between islands; e, the electronic charge; m, the electronic mass; K, the Boltzmann's constant; r, the average radius of islands; ϕ, the potential barrier between islands; h, the Planks constant; ε, the dielectric constant of the substrate and ΔEg, the energy band gap.

In the present case, negative TCR continously decreases with increasing temperature. Therefore, it can be said that contribution towards TCR due to the first term in expression (6) is more predominant compared to the second term. At higher temperatures, it may be possible that contribution from the second term may increase, thus changing the nature of the curve.

With the help of eq. (6), the negative minima and maxima can be explained easily. In certain range of temperature, the term C/T^2, in eq. (6) becomes more predominant. In the present case, it was found to be ~100–150°C. The negative minima and maxima probably depend upon the melting point of the material, nature of the deposit and the conditions of deposition.

4. Conclusion

From the above studies, it appears that thin films of $Bi_{1-x}Sb_x$ formed on glass substrates at room temperature employing three-temperature method, exhibit semiconducting ($0 < x \leq 0.42$) and semiconducting to metallic ($x > 0.42$) behaviours. The activation energy (ΔE) for

semiconducting films have a maxima at a concentration near 5 at.% of Sb. With an increase in concentration of Sb in Bi the band gap in Bi decreases to almost zero at Sb = 42 at.%. The decrease in ΔE with increasing thickness is due to the change in barrier height due to the size of grain in polycrystalline film, large dislocations in crystals, quantum size effect and changes in stoichiometry and also can be explained on the basis of island structure theory. The $Bi_{1-x}Sb_x$ films of intermediate composition have high resistivity with a peak at around 10–20 at.% of Sb, which is probably due to the depletion of carriers in the films.

Temperature coefficient of resistance (TCR) for $Bi_{1-x}Sb_x$ ($0 < x \leq 0.42$) is negative and it decreased with rise in temperature which can be explained on the basis of island structure theory.

References

[1] R B Forst and L R Williams *Proc IIIrd International Conf. on Thermoelectric Energy Conservation* (Arlington, TX, USA) p 139 (1980)

[2] R P Agarawalles, V C George and A K Dua *Jpn J Appl. Phys. Suppl.* 2 p 721 (1974)

[3] Yu V Nikitin, E I Bukhstab and Yu F Komnik *Fiz Nizk Temp.* **4** 1007, 1143, 1257, 1440 (1978)

[4] P Mikolajczak, Subotowicz and R Kleeman *Thin Solid Films* **34** 171 (1976)

[5] Joy George and T I Palson *Thin Solid Films* **127** 233 (1985)

[6] P S Nikam and H S Aher *Indian J Pure Appl Phys* **34** 393 (1996)

[7] P S Nikam and H S Aher *Bull Mater Sci.* **17** 41 (1994)

[8] P S Nikam, R Y Borse and R R Pawar *Bull Mater. Sci* **20** 1015 (1997)

[9] G Charlot *Colorimetric Determination of Elements* (Amsterdam Elsevier) p 167 (1964)

[10] I P Hirde and Y D Temburkar *Indian J Pure Appl. Phys.* **28** 583 (1990)

[11] K N Sharma and K Barua *Thin Solid Films* **144** 41 (1986)

[12] T M Uen, K F Huang, M S Chen and Y S Gou *Thin Solid Films* **158** 69 (1988)

[13] V Damodara Das and D Karunakaran *J Appl Phys* **54** 5252 (1983)

[14] J C Slater *Phys Rev* **103** 1631 (1956)

[15] C A Neugebauer *Z. Angew Phys* **14** 182 (1962), *Phys Thin films* **Vol. 2** (New York : Academic) p 25. (1964)

[16] C A Neugebauer and M B Weeb *J Appl Phys* **33** 74 (1962)

[17] P S Nikam and H S Aher *Indian J Pure Appl. Phys.* **31** 79 (1993)

[18] D S Champbell in *The Use of Thin Films In Physical Investigations* ed J C Anderson (New York : Academic) p 299 (1966)

[19] A F Mayadas and M Shatzkes *Phys Rev* **B1** 1382 (1970)

[20] Yu F Komnik, E I Bukhstab and Yu V Nikitin *Thin Solid Films* **52** 361 (1978)

[21] P S Nikam and D L Mankar *Indian J. Pure Appl Phys.* **21** 361 (1983)